The 7th Indonesia Japan Joint Scientific Symposium (IJJSS 2016)
Chiba, 20-24 November 2016

Topic : Remote Sensing

Phase Coded Stepped Frequency Linear Frequency Modulated Waveform Synthesis Technique for Ultra-Wideband Synthetic Aperture Radar

CHUA Ming Yam[a,*], KOO Voon Chet[a], LIM Heng Siong[a], Chan Yee Kit[a], Josaphat Tetuko Sri Sumantyo[b]

[a]*Faculty of Engineering and Technology, Multimedia University, Jalan Ayer Keroh Lama, 75450 Bukit Beruang, Melaka, Malaysia*

[b]*Josaphat Microwave Remote Sensing Laboratory (JMRSL), Center for Environmental Remote Sensing, Chiba University, 1-33 Yayoi, Inage, Chiba 263-8522 Japan*

Abstract

This paper presents the design work of Phase Coded (PC) Stepped Frequency Linear Frequency Modulated (SF_c-LFM) technique targeted for use in Ultra-Wide Band (UWB) Synthetic Aperture Radar (SAR). The technique is a hybrid approach that employs digital waveform synthesis technique for baseband LFM pulse generation and analogue microwave up-conversion technique. In this work, a train of phase coded baseband LFM pulses is generated using a custom designed Field Programmable Gate Array (FPGA) waveform synthesis board and each baseband pulses are then up-converted to different adjacent band in the carrier band. The collected train of pulses is then re-combined and processed, to synthesis an ultra-wideband pulses. The experimental results show that the technique is able to synthesize a UWB SAR LFM pulse signal. The main advantage of the technique is its capability to improve existing SAR system resolution without having to increase the baseband bandwidth of the system.

Keywords

Keywords: UWB; SAR; Linear FM; Stepped-Frequency; Signal Synthesis.

1. Introduction

SAR is a modern radar system that utilizes pulse compression technique to improve its system resolution whilst maintaining the pulse width of the signal (Skolnik, 1970; Ulaby et. al, 1981). It uses match-filtering technique to compress a wide pulse into a very narrow impulse response (Barton, 1988; Mahafza, 1998). SAR system has stringent requirement in its signal Time Bandwidth Product (TBP). The TBP determines the pulse compression ratio, which is the quantitative measure on the system's range resolution.

Conventionally, a large bandwidth signal can be synthesised using a Voltage Controlled Oscillator (VCO). However, this method is not suitable for SAR signal synthesis as the VCO has a very slow sweep time (Chan and Lim, 2008). On the other hand, due to the limitation in DACs sampling speed, the digital approach is more suitable for low bandwidth (< 100 MHz) signal synthesis applications. Furthermore, increasing the DACs sampling speed introduces new issues in hardware system design, and also increases the

* Corresponding author. Tel.: +85-070-4328-9428
E-mail address: mychua@chiba-u.jp

requirement of Analogue-to-Digital Converter (ADC) sampling speed and system bus data transfer rate.

In order to solve the problem, a new technique on Phase Coded Stepped Frequency Linear FM (SF_c-LFM) method is proposed for Ultra-Wide Band (UWB) SAR signal generation.

2. Phase Coded SF_c-LFM Waveform Synthesis Technique

In traditional, SAR transmits a single burst baseband LFM pulse at every Pulse Repetition Interval (PRI). The transmitted pulse is in its carrier frequency, f_c, given as,

$$x_{tx}(t) = \Pi\left(\frac{t}{T}\right) \cdot e^{j\pi(\alpha t^2 - Bt)} \cdot e^{j2\pi f_c t} \tag{1}$$

In the proposed Phase Coded SF_c-LFM technique, multiple burst of phase coded LFM pulse (or known as intra-pulses) was transmitted, for every SAR PRI interval. They were separated by an intra-PRI interval, t_{pri_int} so that the current listening echo does not overlap with the transmission of the succeeding pulse. Figure 1(a) illustrates an example of the time-frequency plot for 4 burst SF_c-LFM waveform and Figure 1(b) shows an example of the time domain plot of these pulses. Equation below formulates SF_c-LFM signals where each intra-pulses were phase coded.

$$x_{pc}(t_m) = A \cdot \sum_{n=1}^{N} u_b(n) \cdot \prod\left(\frac{t_m}{T}\right) \cdot e^{j\pi(\alpha t_m^2 - Bt_m)} \tag{2}$$

where,

N = number of transmitted pulse within an PRI interval
n = integer number of 1,2,3 … N
$t_m = t - (n-1)t_{pri\_int}$
t_{pri_int} = intra pulse PRI
$u_{b(n)}$ = the implemented phase coding scheme

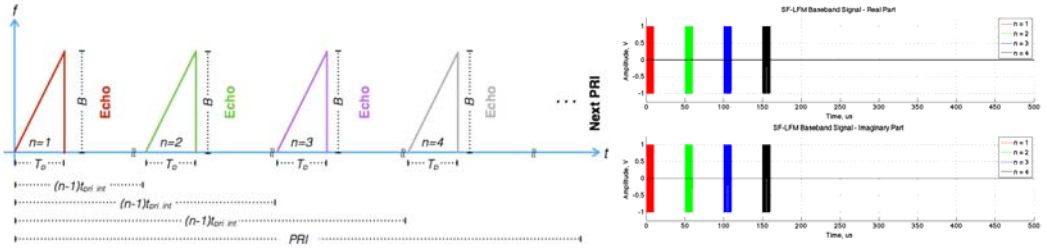

(a) (b)

Figure 1: (a) Time-Frequency Plot for SF_c-LFM (n=4), (b) Time-Domain Plot for SF_c-LFM Baseband Pulses (n=4)

In the proposed technique, each phase coded intra-pulses were mixed with different adjacent carrier frequencies. For design simplicity, an assumption is made that only even number of intra-pulses are transmitted (N is an even number and $N > 2$). Thus, the up-converted signals then can be further expressed as,

$$x_{pc\_rf}(t_m) = A \cdot \sum_{n=1}^{N} u_b(n) \cdot \prod\left(\frac{t_m}{T}\right) \cdot e^{j\pi(\alpha t_m^2 - Bt_m)} \cdot e^{j2\pi f_n t_m} \tag{3}$$

where f_n is the desired adjacent carrier frequency denoted as,

$$f_n = f_c + \left[\left((n-1) - \frac{N}{2}\right) + 0.5\right] B \tag{4}$$

Theoretically, the bandwidth and pulse width are improved N times, where N is the number of transmitted intra-pulses. This infers that the range resolution of a SAR system that employs SF$_c$-LFM scheme signal shall be improved N times. In summary, the effective bandwidth B_{eff}, the effective pulse width T_{eff}, and the effective range resolution ΔR_{eff} are now,

$$B_{eff} = N \times B \tag{5}$$
$$T_{eff} = N \times T_p \tag{6}$$
$$\Delta R_{eff} = \frac{c}{2B_{eff}} \tag{7}$$

Figure 2 depicts the overall up-conversion process of the baseband intra-pulses into its respective adjacent carrier frequency that results in widening its effective bandwidth and pulse width. The intra-pulses in the carrier band are transmitted as in a conventional SAR system. The collected echo is then mixed with its own respective carrier signal to down-convert them into baseband for digitizing and recording. At each intra-pulse interval, t_{pri_int}, a trigger signal is sent to the SAR processor to initiate the recording of the echo pulse. As a result, the SF$_c$-LFM SAR system records N times more echo pulses as compared to a conventional SAR system. It shall be noted that due to the triggering nature in the data acquisition system, the initial point for each collection of digitized echo intra-pulses is zero time referenced.

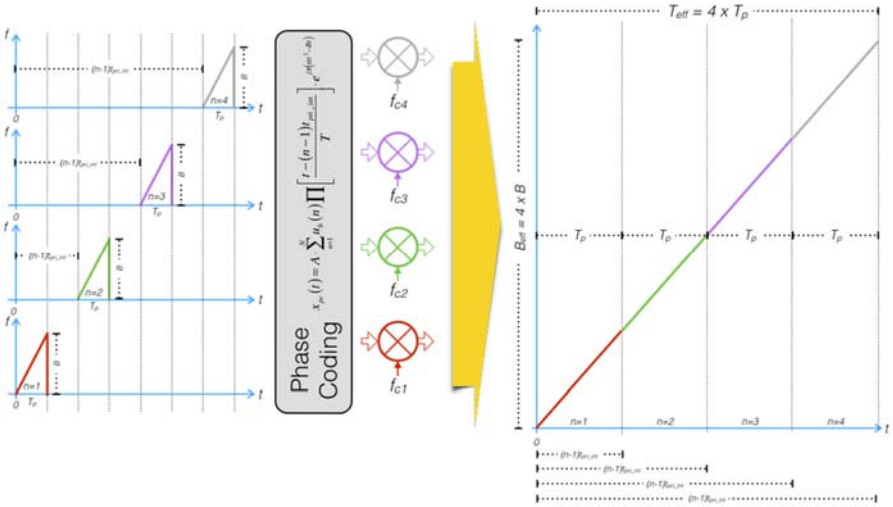

Figure 2: Proposed Phase Coded SF$_c$-LFM Technique

The collected intra-pulses are stored as an array of digital data with N intra-pulses. Before it can be used for SAR image formation, it requires an additional process that employs a dedicated signal re-construction algorithm to merge the recorded data into its equivalent pulse. Theoretically, the re-constructed equivalent pulse shall be,

$$x_{equi}(t) = A \cdot \prod\left(\frac{t}{T_{eff}}\right) \cdot e^{j\pi(\alpha_{eff} t^2 - B_{eff} t)} \tag{8}$$

where,

B_{eff} = Effective bandwidth
T_{eff} = Effective pulse width
α_{eff} = Effective LFM rate = $B_{eff} \times T_{eff}$

Figure 3 shows the signal re-construction process with a record of 4 intra-pulses (N = 4). The received echo for each of the intra-pulses can be formulated as,

$$x_n(t_n) = A_n \cdot u_b(n) \cdot \prod\left(\frac{t_n}{T}\right) \cdot e^{j\pi(\alpha t_n^2 - Bt_n)} \cdot e^{j2\pi f_c t_n} \tag{9}$$

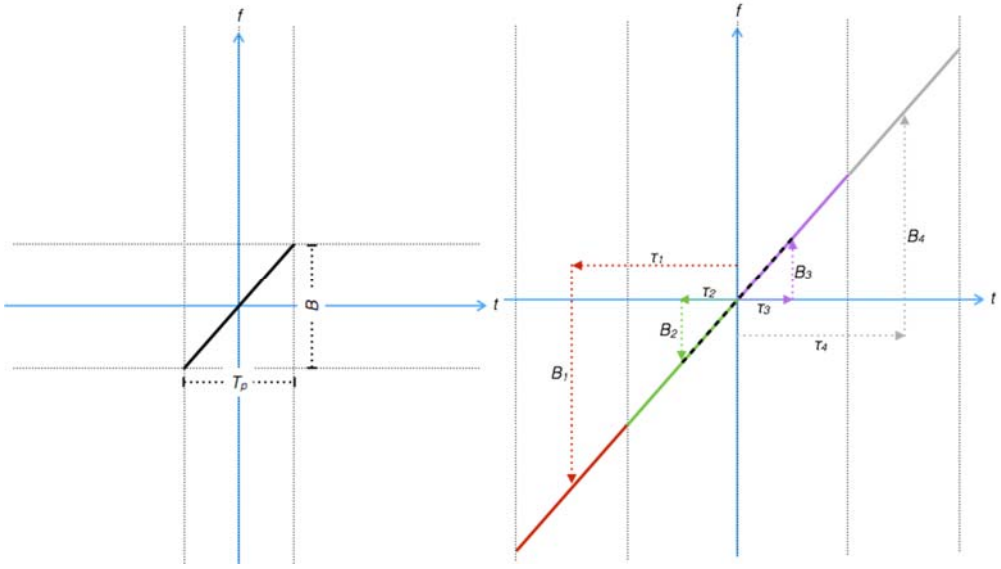

(a) (b)

Figure 3: SF_c-LFM Pulse Reconstruction Algorithm (N = 4): (a) Collected Intra-Pulses Echoes, (b) Signal Reconstruction Algorithm

All of the collected echo intra-pulses will reside at the origin of the time-frequency plot, as shown in the left diagram of Figure 3. In the signal re-construction process, the echo pulses will be re-arranged into their respective frequency bands and time slots. Mathematically, this is by adding a time shift of, τ_n, and a frequency shift of, B_n into each echo intra-pulse. Then, Equation (9) becomes,

$$x_n(t_n - \tau_n) = A_n \cdot u_b(n) \cdot \prod\left(\frac{t_n - \tau_n}{T}\right) \cdot e^{j\pi(\alpha(t_n-\tau_n)^2 - B(t_n-\tau_n)} \cdot e^{j2\pi f_c(t_n-\tau_n)} \cdot e^{j2\pi B_n(t_n-\tau_n)} \tag{10}$$

where,

$$\tau_n = \left[\left((n-1) - \frac{N}{2}\right) + 0.5\right]T \tag{11}$$

$$B_n = \left[\left((n-1) - \frac{N}{2}\right) + 0.5\right]B \tag{12}$$

Solving Equation (10), then, down-converting them to baseband, and finally, removing the additional phase added during the waveform generation, this finally gives,

$$x_n(t_n - \tau_n) = A \cdot \prod\left(\frac{t_n - \tau_n}{T}\right) \cdot e^{j\pi(\alpha t_n^2 - 2\alpha t_n\tau_n - Bt_n + 2B_n t_n + \alpha\tau_n^2 + B\tau_n - 2f_c\tau_n - 2B_n\tau_n)} \tag{13}$$

From Equation (13), it is shown that the phase for each collected intra-pulse echo should be shifted with a time shift, τ_n, and a phase shift with $\emptyset_n$, where $\emptyset_n$ can be quantified as,

$$\emptyset_n = j\pi(-2\alpha t_n\tau_n + 2B_n t_n + \alpha t_n^2 + B\tau_n - 2f_c\tau_n - 2B_n\tau_n) \tag{14}$$

3. FPGA-based Baseband Waveform Synthesizer

An FPGA-based baseband waveform synthesizer was built (Chua and Koo, 2009). In the hardware, it uses Altera Cyclone IV chips as its programmable core with on-board dual-channel, 14-bits, 420 MSPS DAC. Figure 4 shows the custom made FPGA waveform synthesizer board and Table 1 lists the main features of the board. In order to generate the required baseband LFM signals for up-conversion, the board is configured with a real-time re-configurable radar waveform synthesizer as shown in work by Chua *et. al.* (Chua et. al., 2012). Figure 5 depicts the block diagram of the implemented synthesizer.

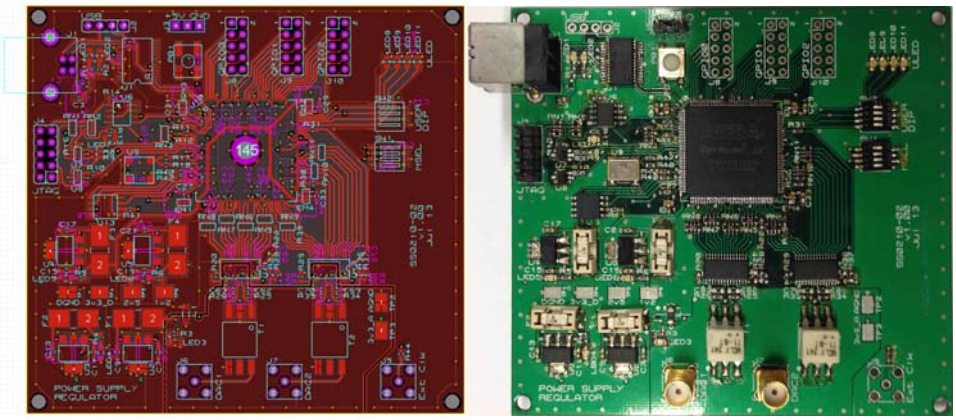

(a) (b)

Figure 4: SF_c-LFM Pulse Reconstruction Algorithm (N = 4): (a) Collected Intra-Pulses Echoes, (b) Signal Reconstruction Algorithm

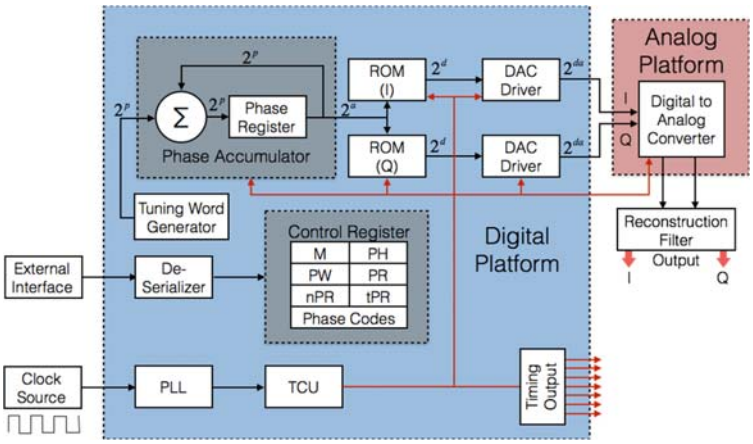

Figure 5: Block Diagram of the Phase Coded SF_c-LFM Waveform Synthesizer

Table 1: Main Features of Custom Designed Altera Cyclone FPGA Board

Module	Specifications
FPGA	– Altera EP4CE22E22C7N – 22,320 LEs – 594 Kbits total memory – 66 18x18-bit multipliers – 4 General Purpose PLLs – 153 user I/Os
DAC	– Analog Device AD9744 DAC – 2 Channel 210 MSPS – 14-bits resolution

4. Experimental Setup

An in-lab proof-of-concept experimental setup was constructed to verify the waveform synthesis technique. Figure 6 illustrates the simplified block diagram of the entire setup.

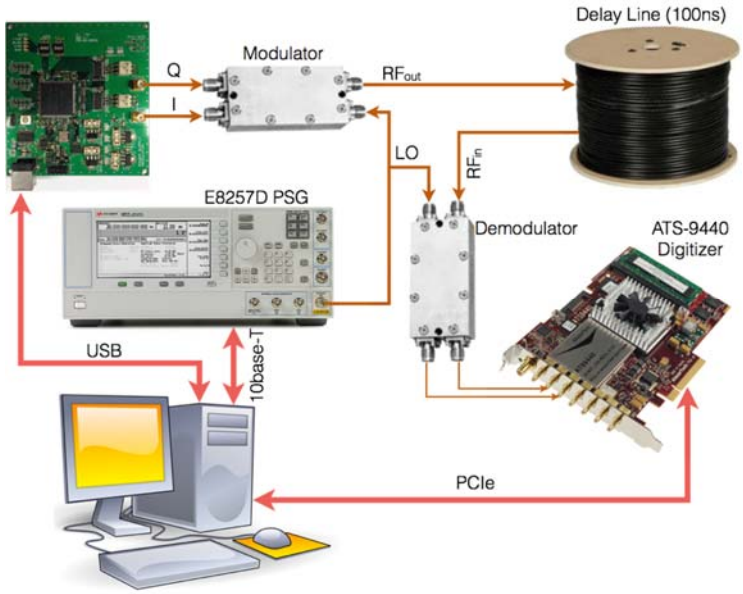

Figure 6: An Illustration of Proof-of-Concept Experimental Setup

In the transmitter, the baseband intra-pulses are up-converted to its respective carrier using an off-the-shelf microwave quadrature modulator. An RF signal generator generates the required stepped carrier signal for the up-conversion. In order to ensure coherency in the transmitted intra-pulses, the selected signal generator has low phase noise (< -120dBc/Hz @ 20 kHz offset) to minimize the phase difference between the intra-pulses. The up-converted intra-pulses are fed into a calibrated microwave delay line for single point target echo emulation. The intra-pulse echoes were then down-converted using an off-the-shelf microwave demodulator and finally these echoes were recorded using an embedded controller with high-speed digitizer.

Table 2: SF_c-LFM Waveform Parameters

Parameters	Value
Number of intra-pulses, N	8
Intra-pulses bandwidth, BW	50 MHz
Pulse Repetition Frequency, PRF	1 kHz
Pulse Width, T_p	10 µs
Carrier Frequency, f_c	2000 MHz
– 1st carrier frequency, f_1	1825 MHz
– 2nd carrier frequency, f_2	1875 MHz
– 3rd carrier frequency, f_3	1925 MHz
– 4th carrier frequency, f_4	1975 MHz
– 5th carrier frequency, f_5	2025 MHz
– 6th carrier frequency, f_6	2075 MHz
– 7th carrier frequency, f_7	2125 MHz
– 8th carrier frequency, f_8	2175 MHz
Effective Bandwidth, B_{eff}	400 MHz
Effective Pulse Width, T_{eff}	10 µs

Table 2 summarizes the SF_c-LFM signal parameters (N = 8). The intra pulses are up-converted to different carrier frequency, $f_1 - f_8$, as depicted in Equation (4). Based on Equation (5) and Equation (6), for the generated SF_c-LFM signal, the effective bandwidth, B_{eff}, is 400 MHz, and the effective pulse width, T_{eff}, is 80 µs.

5. Results and Findings

The spectrum of SF_c-LFM waveform in carrier band are recorded using a spectrum analyzer. Figure 7 shows the recorded frequency spectrum of each of the transmitted intra-pulses and the DSP combined spectrum of the resultant signal.

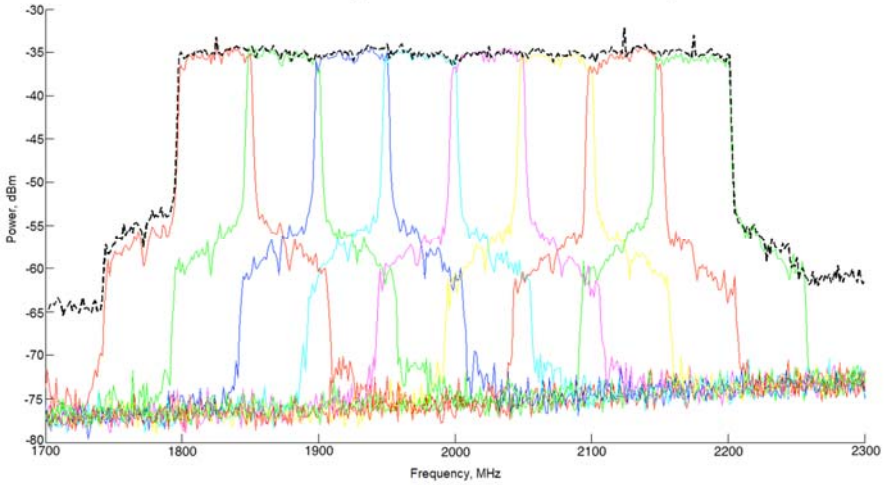

Figure 7: Frequency Spectrum of SF_c-LFM (N = 8, B = 50 MHz): DSP Combined Spectrum (Black colour), Individual Intra-Pulse Spectrum (Other colours)

A phase decoding process (or intra-pulses decryption) is required to remove the phase code added during the baseband waveform generation. Figure 8 illustrates that, without the phase decoding process, the re-constructed pulses will not be able to compress into its equivalent impulse response.

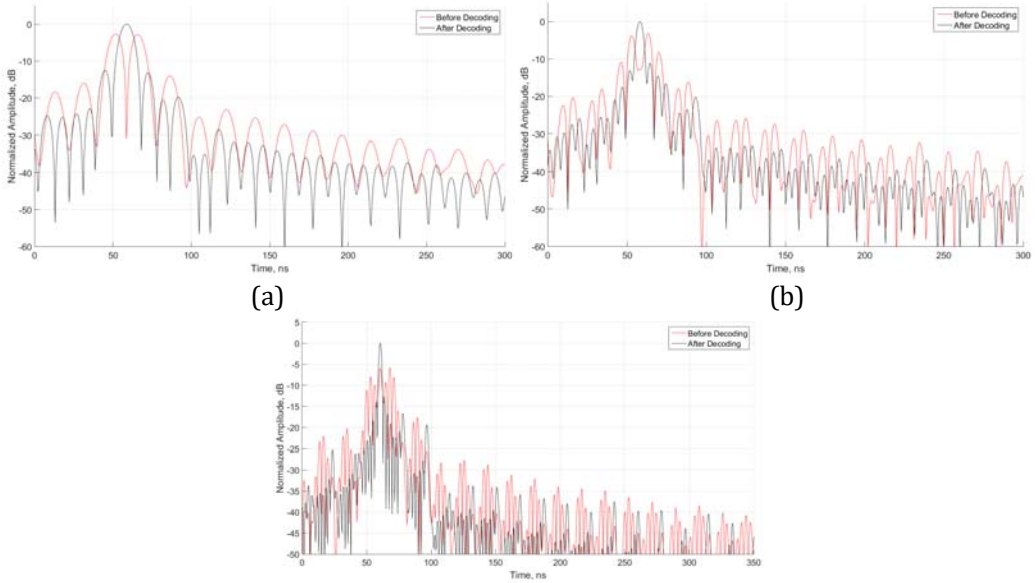

(a) (b)

(c)

Figure 8: Match Filter Output of SF_c-LFM Received Signal; (a) N = 2, (b) N = 4, (c) N = 8.

Figure 9 – Figure 14 show the recorded intra-pulses, the re-constructed pulse and the Auto-Correlation Function (ACF) a.k.a match filter output of the reconstructed pulse. Meanwhile, the measured Peak Side-Lobe Ratio (PSLR) and the Impulse Response Width (IRW) improvement factor obtained for SF_c-LFM waveforms are tabulated in Table 3.

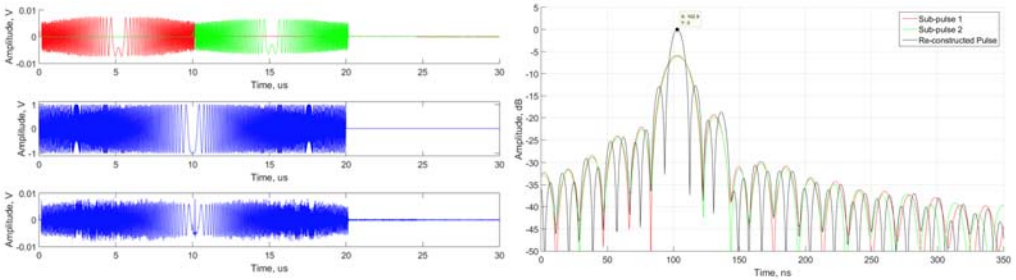

(a) (b)

Figure 9: SF_c-LFM for $N = 2$, $t_d = 100$ns; (a) Top – Intra-Pulses, Middle – Reference Signal, Bottom – Reconstructed Pulse; (b) ACF of the Reconstructed Pulse

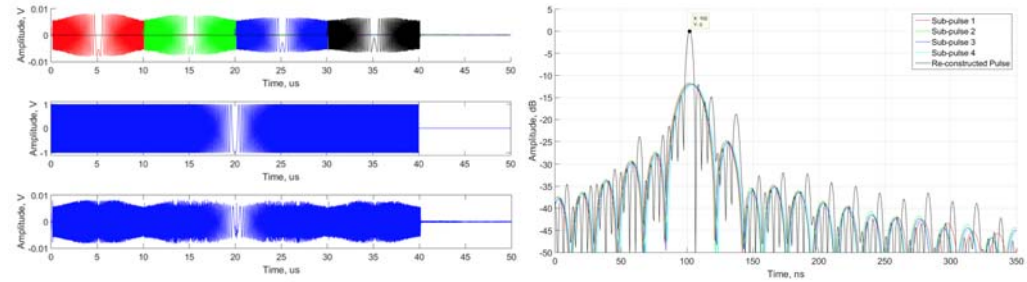

(a) (b)

Figure 10: SF_c-LFM for $N = 4$, $t_d = 100$ns; (a) Top – Intra-Pulses, Middle – Reference Signal, Bottom – Reconstructed Pulse; (b) ACF of the Reconstructed Pulse

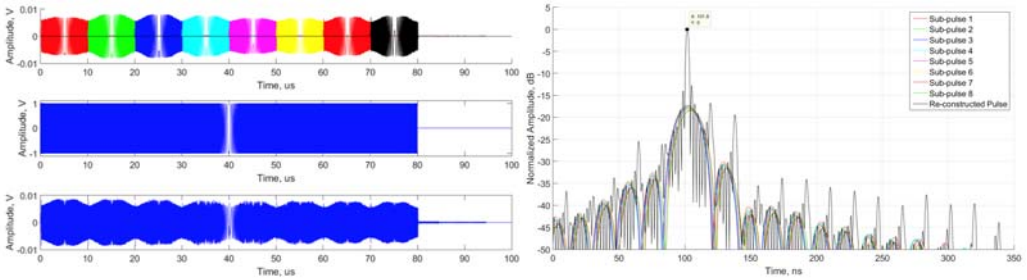

(a) (b)

Figure 11: SF_c-LFM for $N = 8$, $t_d = 100$ns; (a) Top – Intra-Pulses, Middle – Reference Signal, Bottom – Reconstructed Pulse; (b) ACF of the Reconstructed Pulse

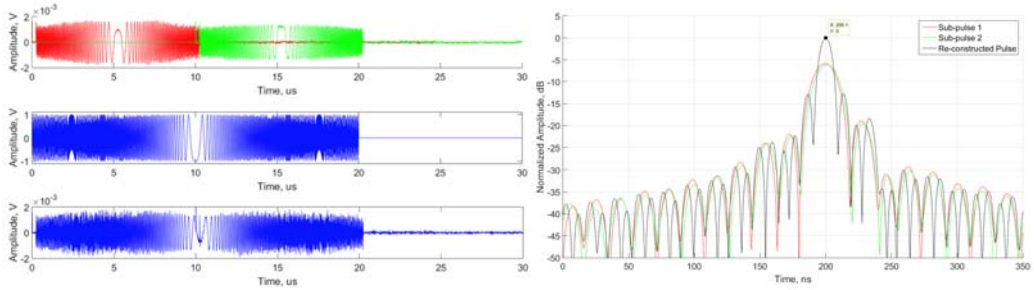

(a) (b)

Figure 12: SF_c-LFM for $N = 2$, $t_d = 200$ns; (a) Top – Intra-Pulses, Middle – Reference Signal, Bottom – Reconstructed Pulse; (b) ACF of the Reconstructed Pulse

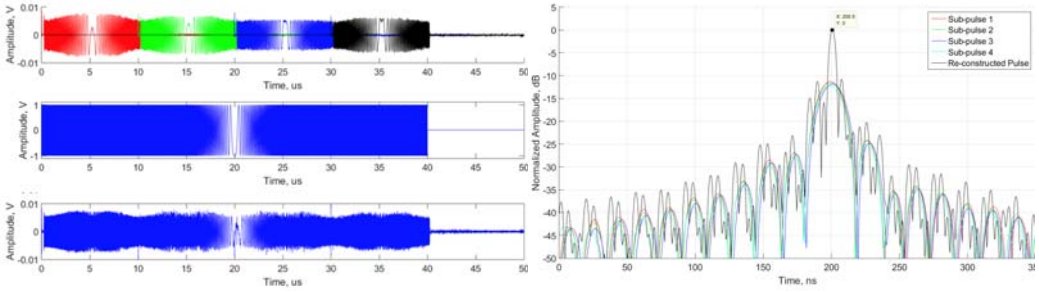

(a) (b)

Figure 13: SF_c-LFM for N = 4, t_d = 200ns; (a) Top – Intra-Pulses, Middle – Reference Signal, Bottom – Reconstructed Pulse; (b) ACF of the Reconstructed Pulse

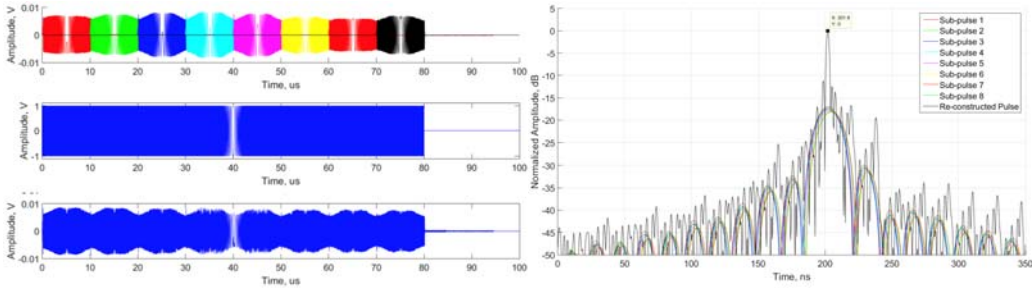

(a) (b)

Figure 14: SF_c-LFM for N = 8, t_d = 200ns; (a) Top – Intra-Pulses, Middle – Reference Signal, Bottom – Reconstructed Pulse; (b) ACF of the Reconstructed Pulse

Table 3: Peak Side-Lobe Ratio Comparison (PSLR) and Improvement in Impulse Response Width (IRW) using SF_c-LFM

Number of intra-pulses *N*	**Delay (*ns*)**	**PSLR (dB)**		**IRW (*ns*)**		**Improvement Factor in IRW (Unit less)**	
		Single-Pulse LFM	**SF_c-LFM**	**Single-Pulse LFM**	**SF_c-LFM**	**Estimated**	**Measured**
2	100	-13.36	-12.89	17.23	8.32	2.00	2.07
	200	-13.11	-12.92	17.23	8.33	2.00	2.07
4	100	-12.96	-12.02	16.70	4.03	4.00	4.14
	200	-12.85	-10.73	16.70	4.01	4.00	4.16
8	100	-12.92	-12.70	16.70	2.00	8.00	8.35
	200	-12.90	-11.25	16.70	1.98	8.00	8.43

6. Conclusion

This paper presents a SF_c-LFM technique to generate UWB SAR LFM signal. The technique can synthesize a greater bandwidth and wider pulse width signal as compared to conventional SAR system. The obtained result has proven that SF_c-LFM technique is able to improve the system range resolution, whilst maintain the required SAR signal quality. Also, the introduction of phase coding scheme into the transmitting signal enhanced the immunity of the radar system on radar system's electronics countermeasure. In conclusion, the proposed waveform modulation technique and its synthesis technique can practically be implemented.

Acknowledgements

This work is funded by the Minister of Higher Education Malaysia (MOHE) under account no 203.PJJAUH.6711279, and Japanese International Cooperation Agency (JICA).

References

Barton D. K. (1988), Modern Radar System Analysis, Norwood, Artech House.

Chan Y. K., Koo V. C. (2008), An Introduction to Synthetic Aperture Radar (SAR), Progress in Electromagnetics Research B, Vol. 2, pp. 27-60.

Chan Y. K., Lim S. Y. (2008), Synthetic Aperture Radar (SAR) Signal Generation, Progress in Electromagnetics Research B, Vol. 1, pp., 269-290.

Chua M. Y., Koo V. C. (2009), "FPGA-based Chirp Generator for High Resolution UAV SAR", PIER99, pp 71-88.

Chua M.Y., Boey H.S., Lim C.H., Koo V.C., Lim H.S., Chan Y.K., Lim T. S. (2012), "A Miniature Real-Time Re-configurable Radar Waveform Synthesizer for UAV based Radar", PIERC2012, Vol. 31, pp. 169-183, 2012.

Mahafza B. F. (1998), Introduction to Radar Analysis, New York, CRC Press.

Skolnik M. I. (1970), Radar Handbook, New York, McGraw-Hill.

Ulaby F. T., Moore R. K., and Fung A. K. (1981), Microwave Remote Sensing: Active and Passive, Vol. 1, Norwood, Artech House.